Table S1 Mouse homozygous knockout phenotypes curated within the MGI

Allelic Composition	*Homozygous*	*Genotype ID*	*Annotated Term*	*Phenotype Summary*	*Referenc*
Lrp1<b2b1554Clo>	Global	MGI:543711	abnormal body wall morphology	growth/size/body region	J:175213
Lrp1<b2b1554Clo>	Global	MGI:543711	abnormal heart ventricle outflow tract morphology	cardiovascular system	J:175213
Lrp1<b2b1554Clo>	Global	MGI:543711	atrioventricular septal defect	cardiovascular system	J:175213
Lrp1<b2b1554Clo>	Global	MGI:543711	diaphragmatic hernia	muscle	J:175213
Lrp1<b2b1554Clo>	Global	MGI:543711	herniated abdominal wall	growth/size/body region	J:175213
Lrp1<b2b1554Clo>	Global	MGI:543711	omphalocele	growth/size/body region	J:175213
Lrp1<tm1.1(KOMP)Wtsi	Global	MGI:563127	abnormal embryo size	embryo	J:211773
Lrp1<tm1.1(KOMP)Wtsi	Global	MGI:563127	abnormal embryo size	growth/size/body region	J:211773
Lrp1<tm1.1(KOMP)Wtsi	Global	MGI:563127	abnormal limb bud morphology	embryo	J:211773
Lrp1<tm1.1(KOMP)Wtsi	Global	MGI:563127	abnormal limb bud morphology	limbs/digits/tail	J:211773
Lrp1<tm1.1(KOMP)Wtsi	Global	MGI:563127	pallor	integument	J:211773
Lrp1<tm1.1(KOMP)Wtsi	Global	MGI:563127	preweaning lethality, complete penetrance	mortality/aging	J:211773
Lrp1<tm1Her>	Global	MGI:218088	embryonic growth retardation	embryo	J:30077
Lrp1<tm1Her>	Global	MGI:218088	embryonic growth retardation	growth/size/body region	J:30077
Lrp1<tm1Her>	Global	MGI:218088	embryonic lethality during organogenesis, complete penetrance	mortality/aging	J:30077
Lrp1<tm1Her>	Global	MGI:218088	internal hemorrhage	cardiovascular system	J:30077
Lrp1<tm2Ajmr>	Global	MGI:383034	abnormal liver morphology	liver/biliary system	J:144146
Lrp1<tm1Her>	Global	MGI:494355	abnormal liver physiology	liver/biliary system	J:76281
Lrp1<tm3Ajmr>	Global	MGI:383035	abnormal liver perisinusoidal space morphology	liver/biliary system	J:144146
Lrp1<tm3Ajmr>	Global	MGI:383035	decreased hepatocyte number	liver/biliary system	J:144146
Lrp1<tm3Ajmr>	Global	MGI:383035	lethality throughout fetal growth and development, incomplete	mortality/aging	J:144146
Lrp1<tm3Ajmr>	Global	MGI:383035	liver degeneration	liver/biliary system	J:144146
Lrp1<tm3Ajmr>	Global	MGI:383035	perinatal lethality, complete penetrance	mortality/aging	J:144146
Lrp1<tm5Ajmr>	Global	MGI:543356	embryonic lethality during organogenesis, complete penetrance	mortality/aging	J:186908
Lrp1<tm2Her> Fabp4-	Adipose	MGI:494373	abnormal adipose tissue amount	adipose tissue	J:127398
Lrp1<tm2Her> Fabp4-	Adipose	MGI:494373	abnormal adipose tissue physiology	adipose tissue	J:127398
Lrp1<tm2Her> Fabp4-	Adipose	MGI:494373	abnormal body temperature homeostasis	homeostasis/metabolism	J:127398
Lrp1<tm2Her> Fabp4-	Adipose	MGI:494373	abnormal brown fat cell morphology	adipose tissue	J:127398
Lrp1<tm2Her> Fabp4-	Adipose	MGI:494373	abnormal circulating lipid level	homeostasis/metabolism	J:127398
Lrp1<tm2Her> Fabp4-	Adipose	MGI:494373	abnormal fat pad morphology	adipose tissue	J:127398
Lrp1<tm2Her> Fabp4-	Adipose	MGI:494373	abnormal glucose homeostasis	homeostasis/metabolism	J:127398
Lrp1<tm2Her> Fabp4-	Adipose	MGI:494373	abnormal lipid homeostasis	homeostasis/metabolism	J:127398
Lrp1<tm2Her> Fabp4-	Adipose	MGI:494373	decreased body surface temperature	homeostasis/metabolism	J:127398
Lrp1<tm2Her> Fabp4-	Adipose	MGI:494373	decreased body weight	growth/size/body region	J:127398
Lrp1<tm2Her> Fabp4-	Adipose	MGI:494373	decreased brown adipose tissue amount	adipose tissue	J:127398
Lrp1<tm2Her> Fabp4-	Adipose	MGI:494373	decreased brown fat cell size	adipose tissue	J:127398
Lrp1<tm2Her> Fabp4-	Adipose	MGI:494373	decreased brown fat lipid droplet number	adipose tissue	J:127398
Lrp1<tm2Her> Fabp4-	Adipose	MGI:494373	decreased circulating free fatty acids level	homeostasis/metabolism	J:127398
Lrp1<tm2Her> Fabp4-	Adipose	MGI:494373	decreased circulating glucose level	homeostasis/metabolism	J:127398
Lrp1<tm2Her> Fabp4-	Adipose	MGI:494373	decreased circulating insulin level	homeostasis/metabolism	J:127398
Lrp1<tm2Her> Fabp4-	Adipose	MGI:494373	decreased circulating leptin level	homeostasis/metabolism	J:127398
Lrp1<tm2Her> Fabp4-	Adipose	MGI:494373	decreased epididymal fat pad weight	adipose tissue	J:127398
Lrp1<tm2Her> Fabp4-	Adipose	MGI:494373	decreased interscapular fat pad weight	adipose tissue	J:127398
Lrp1<tm2Her> Fabp4-	Adipose	MGI:494373	decreased liver triglyceride level	homeostasis/metabolism	J:127398
Lrp1<tm2Her> Fabp4-	Adipose	MGI:494373	decreased liver triglyceride level	liver/biliary system	J:127398
Lrp1<tm2Her> Fabp4-	Adipose	MGI:494373	decreased susceptibility to diet-induced obesity	growth/size/body region	J:127398
Lrp1<tm2Her> Fabp4-	Adipose	MGI:494373	decreased susceptibility to diet-induced obesity	homeostasis/metabolism	J:127398
Lrp1<tm2Her> Fabp4-	Adipose	MGI:494373	decreased total body fat amount	adipose tissue	J:127398
Lrp1<tm2Her> Fabp4-	Adipose	MGI:494373	decreased white fat cell size	adipose tissue	J:127398
Lrp1<tm2Her> Fabp4-	Adipose	MGI:494373	impaired adaptive thermogenesis	homeostasis/metabolism	J:127398
Lrp1<tm2Her> Fabp4-	Adipose	MGI:494373	improved glucose tolerance	homeostasis/metabolism	J:127398
Lrp1<tm2Her> Fabp4-	Adipose	MGI:494373	increased energy expenditure	homeostasis/metabolism	J:127398
Lrp1<tm2Her> Fabp4-	Adipose	MGI:494373	increased food intake	behavior/neurological	J:127398
Lrp1<tm2Her> Fabp4-	Adipose	MGI:494373	increased muscle cell glucose uptake	cellular	J:127398
Lrp1<tm2Her> Fabp4-	Adipose	MGI:494373	increased muscle cell glucose uptake	muscle	J:127398
Lrp1<tm2Her> Fabp4-	Adipose	MGI:494373	increased oxygen consumption	homeostasis/metabolism	J:127398
Lrp1<tm2Her> Fabp4-	Adipose	MGI:494373	increased susceptibility to weight loss	growth/size/body region	J:127398
Lrp1<tm2Her> Fabp4-	Adipose	MGI:494373	trunk curl	behavior/neurological	J:127398
Lrp1<tm2Her> Tagln-cre	Smooth Muscle	MGI:494374	abnormal aorta elastic tissue morphology	cardiovascular system	J:167799
Lrp1<tm2Her> Tagln-cre	Smooth Muscle	MGI:494374	abnormal aorta smooth muscle morphology	cardiovascular system	J:167799
Lrp1<tm2Her> Tagln-cre	Smooth Muscle	MGI:494374	abnormal aorta smooth muscle morphology	muscle	J:167799
Lrp1<tm2Her> Tagln-cre	Smooth Muscle	MGI:494374	abnormal aorta tunica media morphology	cardiovascular system	J:167799
Lrp1<tm2Her> Tagln-cre	Smooth Muscle	MGI:494374	abnormal vascular smooth muscle physiology	cardiovascular system	J:167799
Lrp1<tm2Her> Tagln-cre	Smooth Muscle	MGI:494374	abnormal vascular smooth muscle physiology	muscle	J:167799
Lrp1<tm2Her> Tagln-cre	Smooth Muscle	MGI:494374	abnormal vascular wound healing	cardiovascular system	J:167799
Lrp1<tm2Her> Tagln-cre	Smooth Muscle	MGI:494374	abnormal vascular wound healing	homeostasis/metabolism	J:167799
Lrp1<tm2Her> Tagln-cre	Smooth Muscle	MGI:494374	decreased vasoconstriction	cardiovascular system	J:167799
Lrp1<tm2Her> Tagln-cre	Smooth Muscle	MGI:494374	decreased vasoconstriction	muscle	J:167799
Lrp1<tm2Her> Tagln-cre	Smooth Muscle	MGI:610294	abnormal ascending aorta morphology	cardiovascular system	J:209752
Lrp1<tm2Her> Tagln-cre	Smooth Muscle	MGI:610294	abnormal coronary artery morphology	cardiovascular system	J:209752
Lrp1<tm2Her> Tagln-cre	Smooth Muscle	MGI:610294	abnormal heart echocardiography feature	cardiovascular system	J:209752
Lrp1<tm2Her> Tagln-cre	Smooth Muscle	MGI:610294	abnormal myocardial fiber morphology	cardiovascular system	J:209752
Lrp1<tm2Her> Tagln-cre	Smooth Muscle	MGI:610294	abnormal myocardial fiber morphology	muscle	J:209752
Lrp1<tm2Her> Tagln-cre	Smooth Muscle	MGI:610294	aortic valve regurgitation	cardiovascular system	J:209752
Lrp1<tm2Her> Tagln-cre	Smooth Muscle	MGI:610294	ascending aorta dilation	cardiovascular system	J:209752
Lrp1<tm2Her> Tagln-cre	Smooth Muscle	MGI:610294	cardiac interstitial fibrosis	cardiovascular system	J:209752
Lrp1<tm2Her> Tagln-cre	Smooth Muscle	MGI:610294	decreased cardiac muscle contractility	cardiovascular system	J:209752
Lrp1<tm2Her> Tagln-cre	Smooth Muscle	MGI:610294	decreased cardiac muscle contractility	muscle	J:209752
Lrp1<tm2Her> Tagln-cre	Smooth Muscle	MGI:610294	decreased systemic arterial diastolic blood pressure	cardiovascular system	J:209752
Lrp1<tm2Her> Tagln-cre	Smooth Muscle	MGI:610294	dilated aorta bulb	cardiovascular system	J:209752
Lrp1<tm2Her> Tagln-cre	Smooth Muscle	MGI:610294	dilated cardiomyopathy	cardiovascular system	J:209752
Lrp1<tm2Her> Tagln-cre	Smooth Muscle	MGI:610294	dilated cardiomyopathy	muscle	J:209752
Lrp1<tm2Her> Tagln-cre	Smooth Muscle	MGI:610294	dilated heart left ventricle	cardiovascular system	J:209752
Lrp1<tm2Her> Tagln-cre	Smooth Muscle	MGI:610294	enlarged heart	cardiovascular system	J:209752
Lrp1<tm2Her> Tagln-cre	Smooth Muscle	MGI:610294	enlarged heart	growth/size/body region	J:209752
Lrp1<tm2Her> Tagln-cre	Smooth Muscle	MGI:610294	increased heart left ventricle size	cardiovascular system	J:209752
Lrp1<tm2Her> Tagln-cre	Smooth Muscle	MGI:610294	increased heart weight	cardiovascular system	J:209752
Lrp1<tm2Her> Tagln-cre	Smooth Muscle	MGI:610294	increased heart weight	growth/size/body region	J:209752
Lrp1<tm2Her> Tagln-cre	Smooth Muscle	MGI:610294	increased pulse pressure	cardiovascular system	J:209752
Lrp1<tm2Her> Tagln-cre	Smooth Muscle	MGI:610294	perivascular fibrosis	cardiovascular system	J:209752

Table S2 Homozygous Lrp1$^{tm1.1(KOMP)Wtsi}$ mouse phenotypes.

Procedure	Parameter	pValue	Mice Abnormal	Mice Normal	Total controls
Viability E12.5 Secondary Screen	preweaning lethality, complete penetrance	-	6	0	-
Gross Morphology Embryo E12.5	Embryo Size	0	3	3	1682
Gross Morphology Embryo E12.5	Limb Bud Morphology	0	2	4	1682
Gross Morphology Embryo E12.5	Pallor	0	2	4	1682
Gross Morphology Embryo E12.5	Pericardium Morphology	0	2	4	1682
Gross Morphology Embryo E12.5	Delayed embryonic development	1	1	5	1682
Gross Morphology Embryo E12.5	Neural Tube Closure	1	0	6	1671
Gross Morphology Embryo E12.5	Microphthalmia	1	0	4	1550
Gross Morphology Embryo E12.5	Blebs	1	0	6	1682
Gross Morphology Embryo E12.5	Ear Morphology	1	0	6	1682
Gross Morphology Embryo E12.5	Forebrain morphology	1	0	6	1682
Gross Morphology Embryo E12.5	Heart looping	1	0	6	1682
Gross Morphology Embryo E12.5	Anophthalmia	1	0	4	1550
Gross Morphology Placenta E12.5	Placenta Development	1	0	7	1575
Gross Morphology Embryo E12.5	Visceral yolk sac morphology	1	0	6	1682
Gross Morphology Embryo E12.5	Microcephaly	1	0	6	1667
Gross Morphology Embryo E12.5	Facial cleft	1	0	6	1682
Gross Morphology Placenta E12.5	Placenta Morphology	1	0	7	1575
Gross Morphology Embryo E12.5	Pale yolk sac	1	0	6	1682
Gross Morphology Embryo E12.5	Midbrain morphology	1	0	6	1671
Gross Morphology Embryo E12.5	Hindbrain morphology	1	0	6	1682
Gross Morphology Placenta E12.5	Placenta Vasculature	1	0	7	1575
Gross Morphology Embryo E12.5	Head shape	1	0	6	1670
Gross Morphology Embryo E12.5	Abdominal wall	1	0	6	1682
Gross Morphology Embryo E12.5	Pale Liver	1	0	6	1682
Gross Morphology Embryo E12.5	Edema	1	0	6	1682
Gross Morphology Embryo E12.5	Tail Morphology	1	0	6	1682
Gross Morphology Placenta E12.5	Placenta Size	1	0	7	1575
Gross Morphology Placenta E12.5	Umbilical cord morphology	1	0	7	1575
Gross Morphology Embryo E12.5	Craniofacial morphology	1	0	6	1667
Gross Morphology Embryo E12.5	Hemorrhage	1	0	6	1682

Table S3 Heterozygous Lrp1$^{tm1.1(KOMP)Wtsi}$ significant mouse phenotypes.

Procedure	Parameter	Female pValue	Male pValue	Combined pValue
Clinical Chemistry	Alkaline phosphatase	1.10E-04	6.30E-03	1.82E-05
Clinical Chemistry	Triglycerides	6.36E-01	2.38E-05	2.38E-05
Heart Weight	Heart weight	7.74E-05	6.03E-04	7.74E-05
Plasma Chemistry	Triglycerides	4.31E-03	4.73E-03	1.08E-04
Electrocardiogram (ECG)	PR	3.90E-04	1.94E-01	3.90E-04
Electrocardiogram (ECG)	PQ	5.55E-04	1.25E-01	5.55E-04
Clinical Chemistry	Glucose	4.02E-02	2.53E-03	6.27E-04
Eye Morphology	Lens	2.02E-03	4.15E-02	6.55E-04
Sleep Wake	Peak wake with respect to dark onset median	1.55E-02	1.03E-02	7.13E-04
Open Field - centre start	Periphery average speed	1.52E-03	5.08E-01	7.52E-04
Electrocardiogram (ECG)	ST	1.03E-02	2.41E-02	1.04E-03
Open Field - centre start	Center distance travelled	1.30E-03	3.53E-03	1.47E-03
Grip Strength	Forelimb grip strength normalised against body weight	1.46E-03	1.55E-01	2.63E-03
Hole-board Exploration	Total holepokes	9.52E-02	3.66E-03	1.71E-03
Open Field - centre start	Number of rears - total	1.92E-03	7.86E-01	1.92E-03
Electrocardiogram (ECG)	HR	1.19E-02	3.46E-02	2.28E-03
Open Field - centre start	Whole arena average speed	4.00E-03	2.17E-01	2.32E-03
Open Field - centre start	Distance travelled - total	4.13E-03	2.14E-01	2.40E-03
Open Field - centre start	Whole arena resting time	3.98E-03	2.97E-01	2.40E-03
Electrocardiogram (ECG)	CV	1.86E-02	3.54E-02	2.96E-03
Electrocardiogram (ECG)	RR	1.48E-02	4.70E-02	3.71E-03
Eye Morphology	Vitreous	1.00E+00	3.95E-03	2.08E-02
Body Composition (DEXA lean/fat)	Lean mass	4.08E-03	8.14E-01	5.95E-03
Plasma Chemistry	Free fatty acids	3.57E-02	4.42E-02	5.10E-03
Eye Morphology	Fusion between cornea and lens	9.03E-03	1.00E+00	5.22E-03
Electrocardiogram (ECG)	rMSSD	1.20E-02	7.87E-02	5.77E-03
Eye Morphology	Eye	7.40E-03	1.00E+00	7.56E-03
Electrocardiogram (ECG)	HRV	3.70E-02	5.80E-02	1.05E-02
Sleep Wake	Sleep daily percent	7.16E-01	1.17E-02	3.76E-02
Grip Strength	Forelimb grip strength measurement mean	2.75E-02	1.03E-01	1.34E-02
Eye Morphology	Pupil Dilation	1.40E-02	1.00E+00	2.87E-02
Light-Dark Test	Percent time in dark	1.76E-02	3.97E-01	1.45E-02
Light-Dark Test	Percent time in light	1.76E-02	3.97E-01	1.45E-02
Open Field - centre start	Percentage center time	1.60E-02	1.32E-01	2.13E-02
Open Field - centre start	Center permanence time	1.60E-02	1.32E-01	2.13E-02
Body Composition (DEXA lean/fat)	Lean/Body weight	1.73E-02	7.73E-01	1.78E-02
Eye Morphology	Pupil Light Response	1.79E-02	1.00E+00	1.92E-02
Light-Dark Test	Dark side time spent	2.31E-02	6.84E-01	2.64E-02
Light-Dark Test	Light side time spent	2.31E-02	6.84E-01	2.64E-02
Open Field - centre start	Periphery distance travelled	4.49E-02	9.34E-01	2.82E-02
Light-Dark Test	Time mobile light side	3.43E-02	1.17E-01	3.43E-02
Sleep Wake	Sleep light phase percent	3.93E-01	3.47E-02	3.80E-02
Acoustic Startle and Pre-pulse Inhibition (PPI)	Response amplitude - S	2.30E-01	4.33E-02	4.93E-02
Body Composition (DEXA lean/fat)	Bone Mineral Content (excluding skull)	4.46E-02	9.07E-01	4.97E-02

Table S4 *LRP1* human correlated genes from Human Protein Atlas linked to OMIM syndromes.

Gene	Correlation to LRP1	Group	Phenotype
SH3PXD2B	0.8614	HPA Tissue cluster	Frank-ter Haar syndrome, Autosomal recessive
MFAP5	0.7843	HPA single cell cluster	Aortic aneurysm, familial thoracic 9, Autosomal dominant
GSC	0.7885	HPA single cell cluster	Short stature, auditory canal atresia, mandibular hypoplasia, skeletal abnormalities, Autosomal recessive
TGFB3	0.8754	HPA Tissue cluster	Arrhythmogenic right ventricular dysplasia 1, Loeys-Dietz syndrome 5, Autosomal dominant
MYOC	0.8343	HPA single cell cluster	Glaucoma 1A, primary open angle, Autosomal dominant
PDGFRL	0.8228	HPA single cell cluster	Hepatocellular cancer, somatic; Colorectal cancer, somatic
GSN	0.8148	HPA single cell cluster	Amyloidosis, Finnish type, Autosomal dominant
TNXB	0.8058	HPA single cell cluster	Ehlers-Danlos syndrome, classic-like, Autosomal recessive
ADCY3	0.9088	HPA Tissue cluster	Obesity, susceptibility to, Autosomal recessive
BOC	0.8525	HPA single cell cluster	none
VIT	0.8466	HPA single cell cluster	none
GAS1	0.8407	HPA single cell cluster	none
MAP1LC3C	0.8054	HPA single cell cluster	none
FBLN2	0.8037	HPA single cell cluster	none
PODN	0.7937	HPA single cell cluster	none
HTRA3	0.7894	HPA single cell cluster	none
PCOLCE2	0.7852	HPA single cell cluster	none
LRRN4CL	0.7828	HPA single cell cluster	none
GFPT2	0.9281	HPA Tissue cluster	none
COL5A3	0.9	HPA Tissue cluster	none
GYG2	0.893	HPA Tissue cluster	none
PAMR1	0.8842	HPA Tissue cluster	none
SEMA4C	0.8789	HPA Tissue cluster	none
COLEC12	0.8684	HPA Tissue cluster	none
TMEM132C	0.8667	HPA Tissue cluster	none
ACVR1C	0.8649	HPA Tissue cluster	none
FGF2	0.8579	HPA Tissue cluster	none
ADAMTS4	0.8561	HPA Tissue cluster	none
GPR146	0.8526	HPA Tissue cluster	none
KCNE4	0.8456	HPA Tissue cluster	none

Table S5 Traits significantly associated with *LRP1* eQTL rs11172113.

Study ID	Trait	Lead Variant P-value	PMID	Study N
GCST011062	Migraine and/or pulse pressure	2.00E-50	32632093	1,094,154
GCST003720	Migraine	6.00E-49	27322543	375,752
GCST005337	Headache	5.00E-47	29397368	223,782
NEALE2_6159_1	Headache | pain type(s) experienced in last month	8.33E-46		360,391
GCST003986	Migraine	6.00E-36	27182965	283,985
GCST007080	Lung function (FEV1/FVC)	6.00E-29	30595370	370,000
NEALE2_20002_1265	Migraine | non-cancer illness code, self-reported	3.99E-24		361,141
GCST007431	Lung function (FEV1/FVC)	7.04E-21	30804560	400,052
GCST002081	Migraine	4.00E-19	23793025	118,710
NEALE2_6154_3	Paracetamol | medication for pain relief, constipation, heartburn	9.84E-19		357,084
GCST011056	Migraine without aura and/or pulse pressure	2.00E-17	32632093	1,094,154
NEALE2_6154_100	None of the above | medication for pain relief, constipation, heartburn	3.92E-17		357,084
GCST003721	Migraine without aura	4.00E-16	27322543	147,790
GCST007938	Medication use (anilides)	9.00E-16	31015401	179,810
FINNGEN_R5_MIGRAINE_TRIPTAN	Migraine	1.00E-15		218,792
NEALE2_20003_2038460150	Paracetamol | treatment/medication code	1.10E-14		361,141
GCST010722	Spontaneous coronary artery dissection	1.00E-13	32374345	2,484
NEALE2_6154_2	Ibuprofen (e.g. nurofen) | medication for pain relief, constipation, heartburn	1.15E-13		357,084
GCST007939	Medication use (antimigraine preparations)	3.00E-13	31015401	119,844
NEALE2_3799	Headaches for 3+ months	1.01E-12		70,181
GCST007800	Asthma (childhood onset)	1.20E-12	30929738	561,282
GCST90000027	Appendicular lean mass	4.20E-11	33097823	244,730
GCST002078	Migraine without aura	1.00E-10	23793025	76,534
GCST011059	Migraine with aura and/or pulse pressure	2.00E-10	32632093	1,094,154
GCST007430	Peak expiratory flow	3.25E-10	30804560	345,265
NEALE2_20003_1140871310	Ibuprofen | treatment/medication code	1.96E-09		361,141
GCST001105	Migraine	4.00E-09	21666692	41,007
GCST001248_2	Pulmonary function [FEV1/FVC]	1.00E-08	21946350	94,612
GCST001563	Migraine	3.00E-08	22683712	12,066
GCST90000582	Spontaneous coronary artery dissection	3.00E-08	32887874	8,903

Table S6 LRP1 linked toxicogenomics from the CTDbase.

Chemical Name	Chemical ID	CAS RN	Interaction Count	Organism Count
bisphenol A	C006780	80-05-7	10	3
Tetrachlorodibenzodioxin	D013749	1746-01-6	8	2
Copper	D003300	7440-50-8	7	2
Acetaminophen	D000082	103-90-2	4	3
Rosiglitazone	D000077154		5	2
Capsaicin	D002211	404-86-4	9	1
Tetradecanoylphorbol Acetate	D013755	16561-29-8	4	2
Tobacco Smoke Pollution	D014028		4	2
Aflatoxin B1	D016604	1162-65-8	3	2
Benzo(a)pyrene	D001564	50-32-8	3	2
Carbon Tetrachloride	D002251	56-23-5	3	2
Cyclosporine	D016572	59865-13-3	3	2
Diethylnitrosamine	D004052	55-18-5	3	2
Dronabinol	D013759		3	2
Ethinyl Estradiol	D004997	57-63-6	3	2
Thioacetamide	D013853	62-55-5	3	2
Ethanol	D000431	64-17-5	5	1
Plant Preparations	D028321		5	1
Cisplatin	D002945	15663-27-1	4	1
Dexamethasone	D003907	50-02-2	4	1
Air Pollutants	D000393		2	2
bis(4-hydroxyphenyl)sulfone	C543008	80-09-1	2	2
Cadmium Chloride	D019256	10108-64-2	2	2
Oxygen	D010100	7782-44-7	2	2
sodium arsenite	C017947	13768-07-5	2	2
Valproic Acid	D014635	99-66-1	2	2
1-Methyl-3-isobutylxanthine	D015056	28822-58-4	3	1
Indomethacin	D007213	53-86-1	3	1
tanshinone	C021751	568-73-0	3	1
Aluminum Chloride	D000077410		2	1

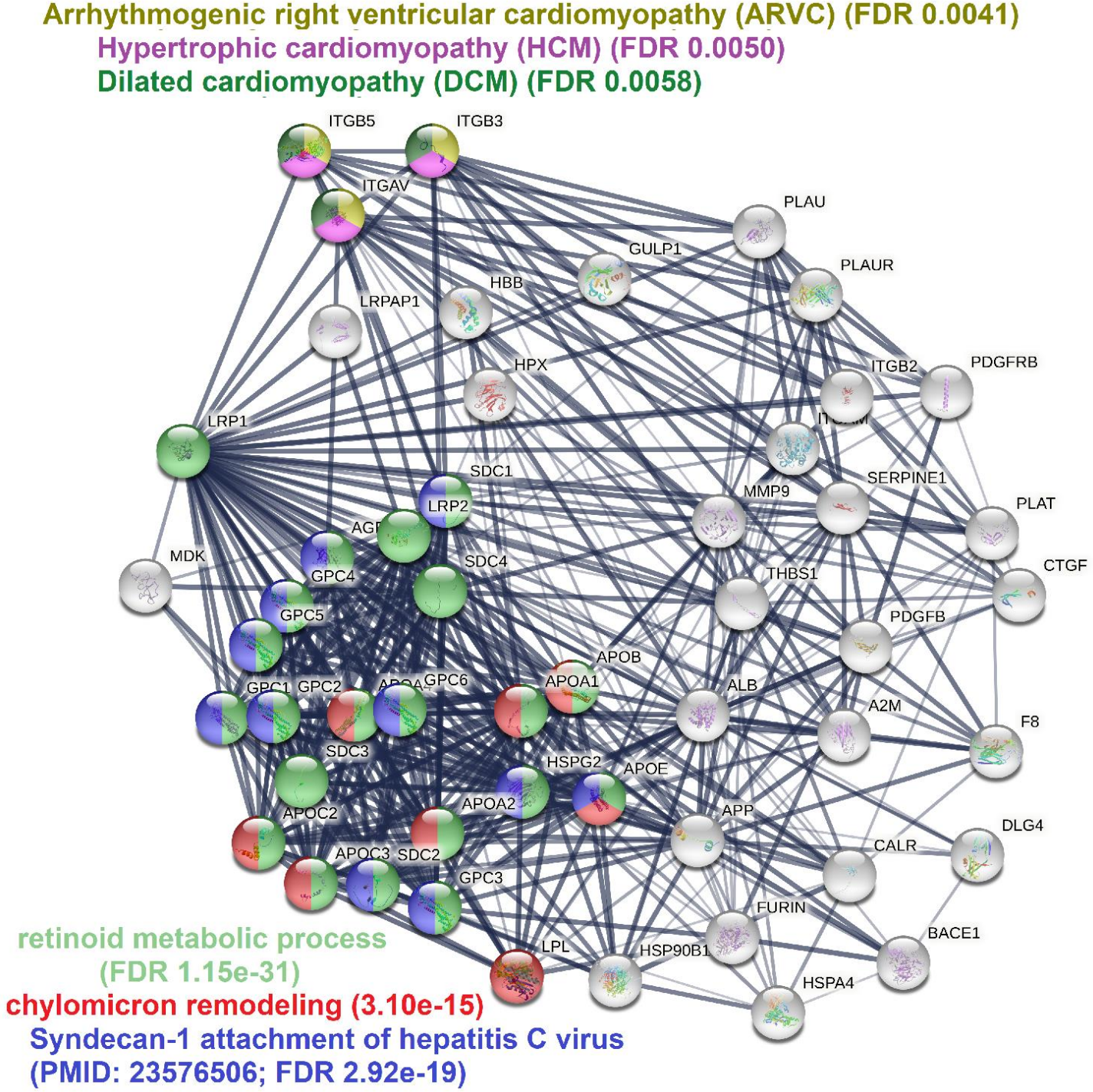

Figure S1 STRING insights for LRP1 protein-interacting network. Colored genes are enriched for the labeled gene ontology term based on the false discovery rate (FDR). Interaction partners are shown based on database interactions, experimental insights, and textmining where the width of the line connecting any two nodes based on strength of correlation. Map was created with https://string-db.org/.

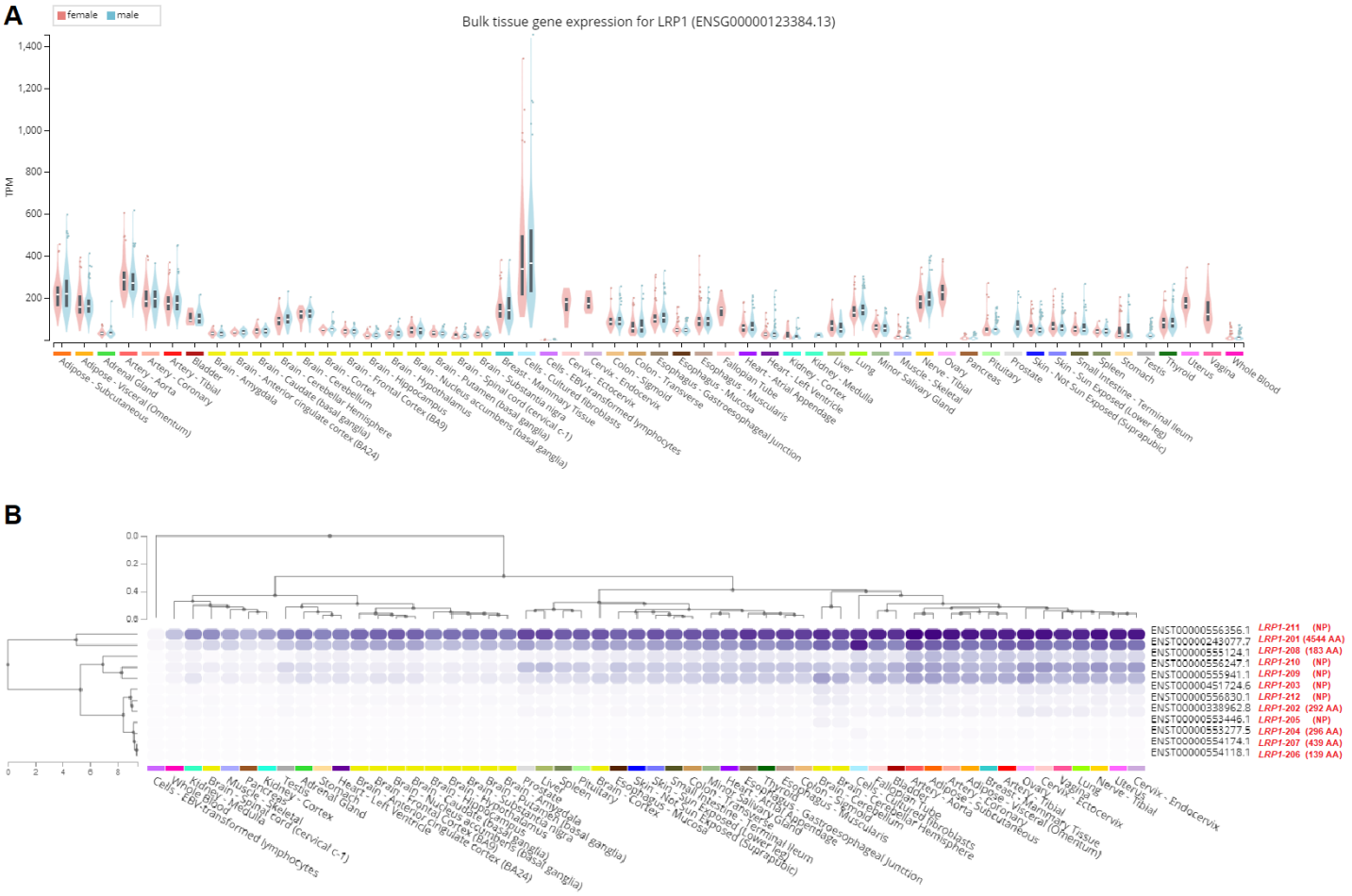

Figure S2 Sex differences in expression of *LRP1* between males and females based on GTEx data. A) Tissue expression of *LRP1* shown as transcripts per million (TPM) for female (red) or male (blue). Data is plotted as a violin plot of diversity for multiple human samples. **B)** Isoforms of *LRP1* expressed in human tissues. The darker blue represents a higher expression. In red are the numbered isoforms with the number of amino acids coded by the transcript or if it does not code for a protein (NP).

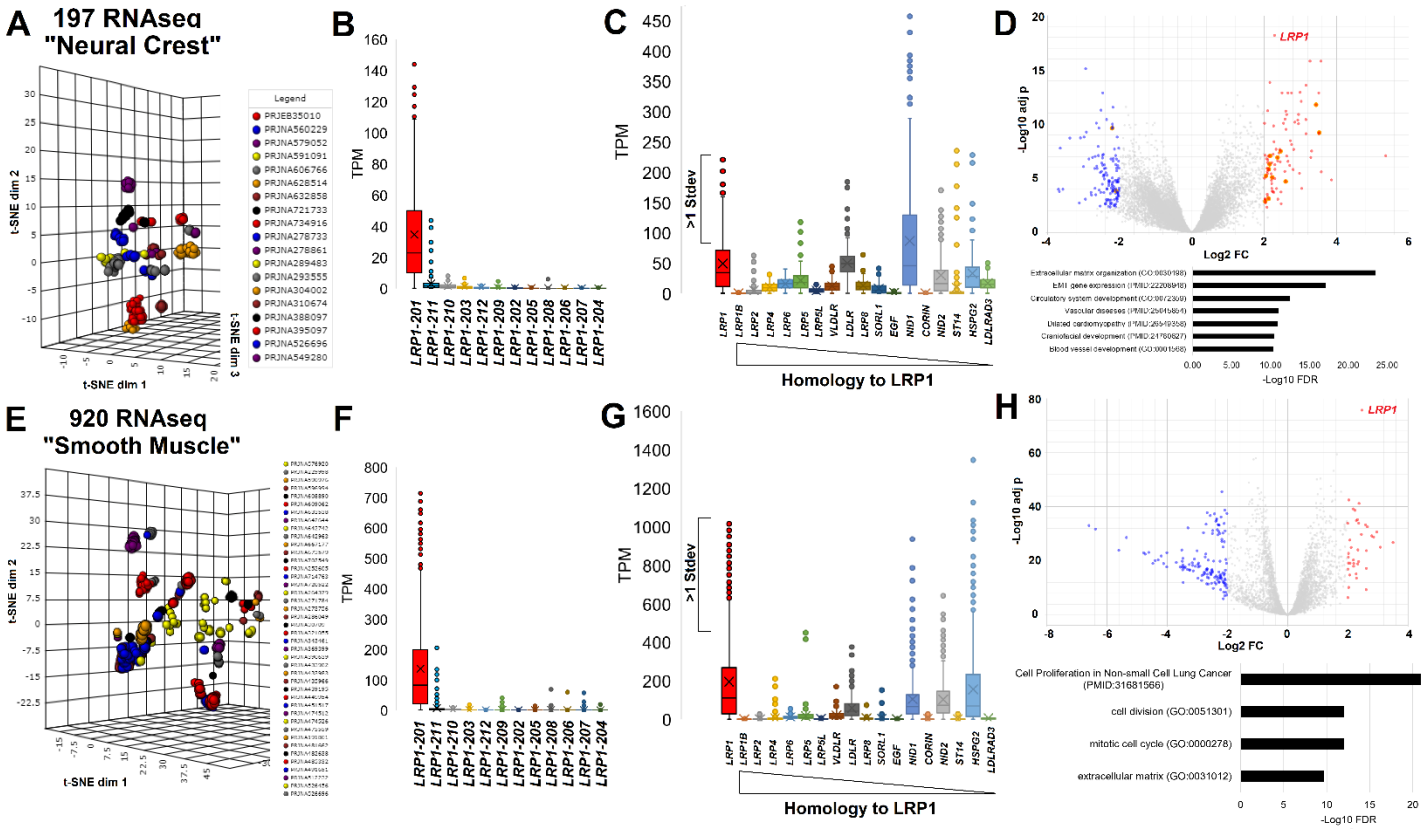

Figure S3 *LRP1* expression to phenotypic insights in neural crest-derived cell types. A-H) Neural crest based RNAseq for 197 datasets (**A-D**) or 920 smooth muscle (**E-H**) showing a three-dimensional principal component plot (**A**/**E**), *LRP1* transcript annotations as a box and whisker plot (**B**/**F**), gene-level expression for each gene shown as a box and whisker plot (**C**/**G**), and genes that are significantly different in *LRP1* expression >1 standard deviation datasets shown as a volcano plot with relevant enriched terms listed below (**D**/**H**). Raw processed data for neural crest RNAseq can be found at https://doi.org/10.6084/m9.figshare.14920644.v1 and the smooth muscle RNAseq at https://doi.org/10.6084/m9.figshare.14991444.v1.

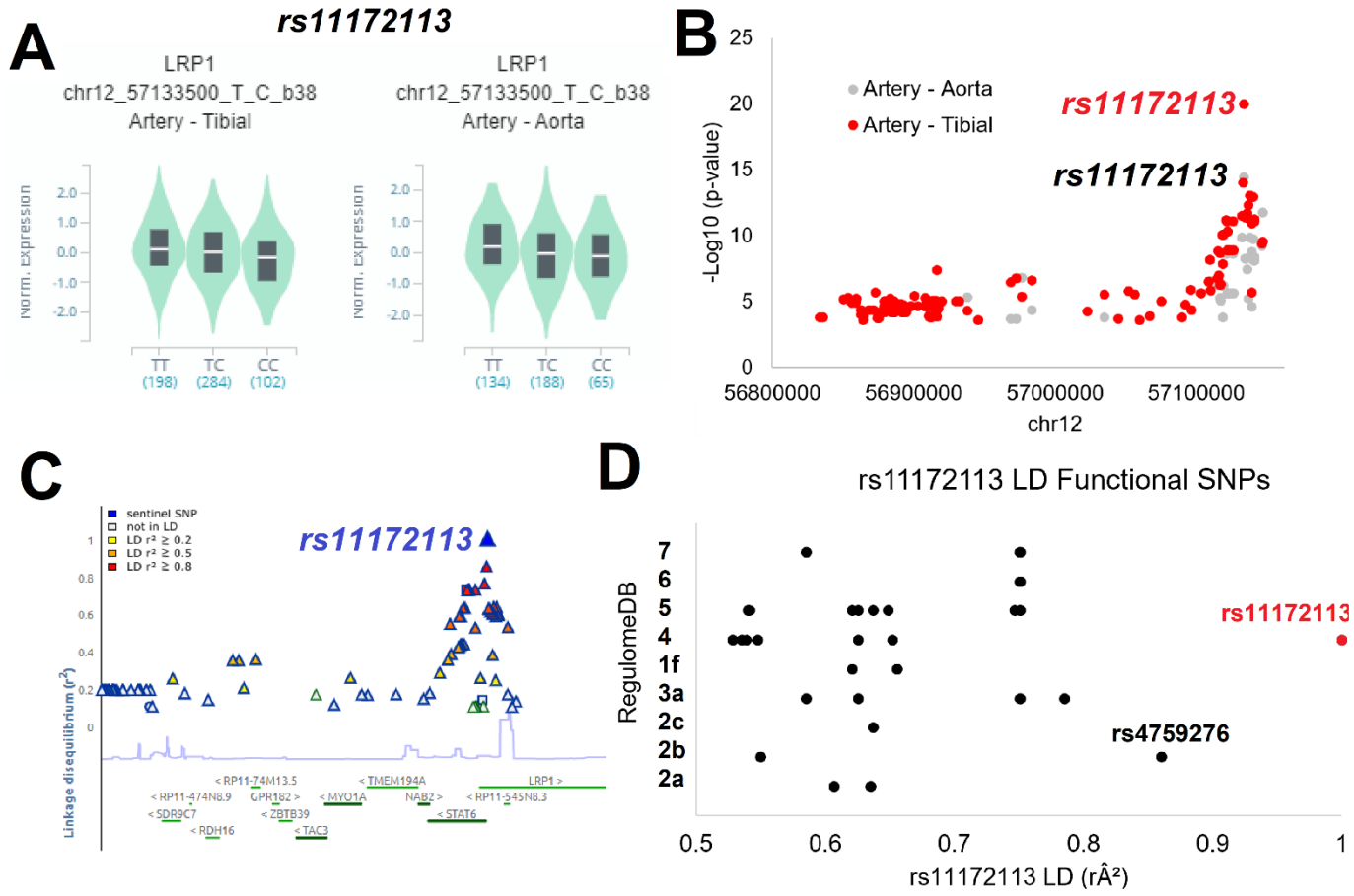

Figure S4 GWAS loci association with vascular phenotypes and *LRP1* expression. **A)** Violin plot of rs11172113 for *LRP1* expression in tibial (left) or aorta (right) artery for homozygous or heterozygous individuals. **B)** Plot of variant associations (y-axis) in the aorta (gray) or tibial (red) artery for *LRP1* expression relative to chromosome 12 location (x-axis). **C)** Linkage disequilibrium (LD) SNPs (y-axis) with rs11172113 relative to gene positions on chromosome 12 (x-axis). **D)** Functional gene regulation knowledge from RegulomeDB (y-axis) for SNPs in LD with rs11172113 (x-axis). The lower the value on the Y-axis, the more knowledge that is present for gene regulation potential.

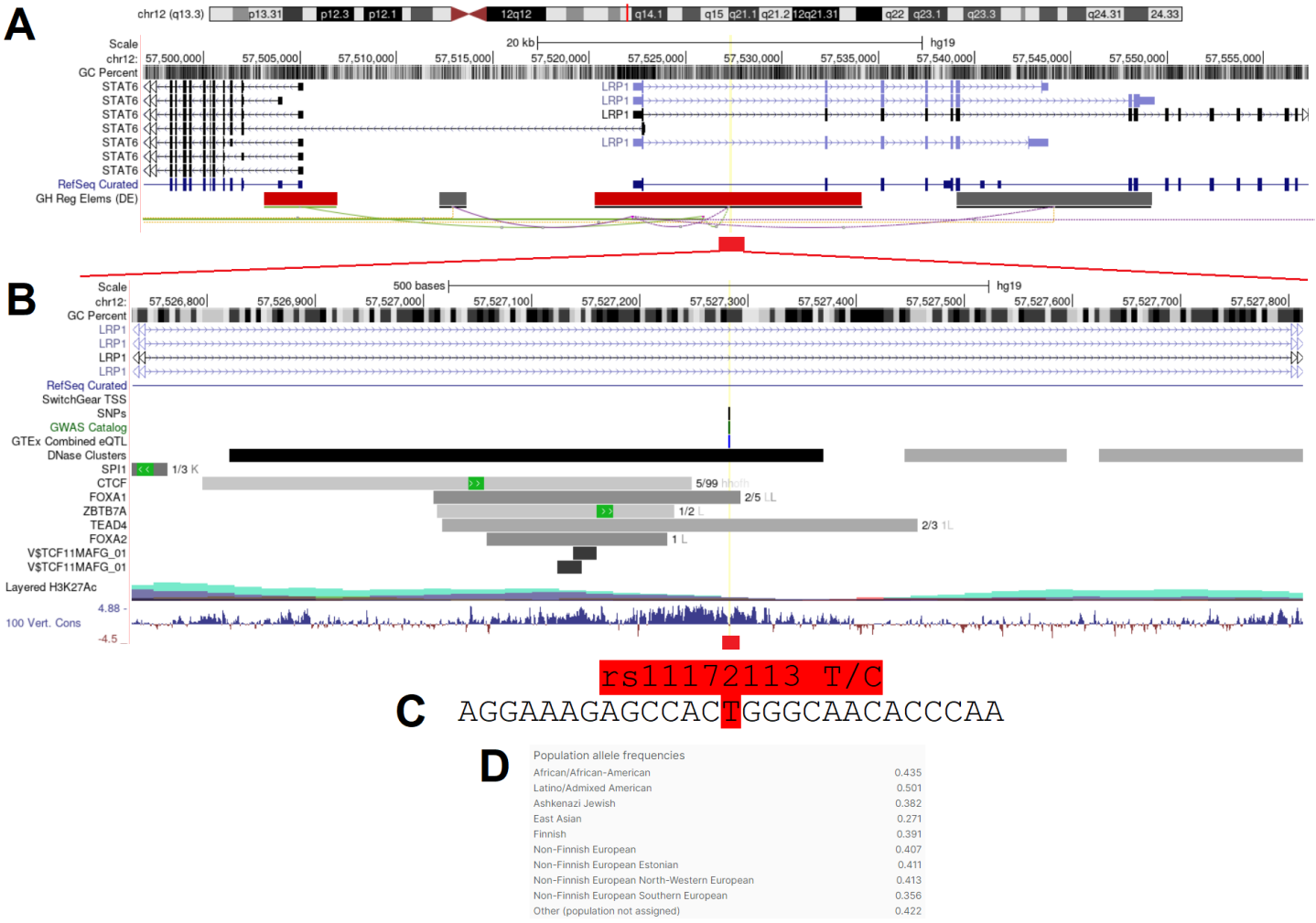

Figure S5 Genome browser view of rs11172113 within an intron of LRP1. **A)** View of the rs11172113 (yellow line) variant relative to exons of LRP1 and STAT6. Shown below the genes are the GeneHancer annotated enhancers with known looping data connecting the sites. **B**) A zoom-in view of the variant showing transcription factor regulation sites and conservation. Any listed protein shows known ChIP-Seq binding peaks at those locations. **C**) Sequence with the variant highlighted in red. **D**) Population allele frequencies based on gnomAD data.